Phonon-Based Calculation of Graphene's Heat Capacity

Ethan Furman*
Department of Physics, Haverford College,
Department of Physics, Bryn Mawr College
Fall 2025

(Dated: March 15, 2026)

We present a phonon-based calculation of graphene's heat capacity using a simple harmonic lattice model of the honeycomb structure. Starting from a nearest-neighbor force-constant description, we construct the dynamical matrix, compute the phonon dispersion relations, and evaluate the heat capacity by summing over phonon modes with Bose–Einstein statistics. Two models are compared: a planar model allowing only in-plane vibrations and a full three-dimensional model including out-of-plane flexural modes. We show that the quadratic dispersion of the flexural acoustic (ZA) branch leads to enhanced low-temperature heat capacity with characteristic T^2 scaling, while purely harmonic models systematically overestimate the room-temperature heat capacity relative to experiment due to neglected anharmonic effects.

I. INTRODUCTION

Graphene is a two-dimensional crystal consisting of a single layer of carbon atoms arranged in a honeycomb lattice. Because it is a 2D material and has strong covalent bonding, graphene exhibits special dynamical and thermal properties that differ from those of conventional three-dimensional solids. In particular, thermal transport and thermodynamic behavior in graphene are dominated by lattice vibrations (phonons), while electronic contributions to the heat capacity are negligible over a wide temperature range.

From a theoretical perspective, graphene provides a clean platform for studying how phonon dispersion relations determine macroscopic thermodynamic properties. Of special importance are the out-of-plane flexural acoustic (ZA) modes, which possess a quadratic dispersion relation near the Brillouin-zone center. This nonstandard dispersion enhances the density of low-frequency states and leads to unconventional low-temperature heat-capacity scaling in two-dimensional membranes.

In this work, we compute graphene's heat capacity directly from its phonon spectrum using a minimal harmonic lattice model. The goal is not quantitative precision, but rather to isolate the role of different phonon branches, especially the ZA mode, and to assess the strengths and limitations of a purely harmonic description.

II. METHODS

A. Honeycomb lattice and degrees of freedom

Graphene's honeycomb lattice contains two carbon atoms per primitive unit cell, conventionally labeled A and B. In the most general case, each atom can vibrate in three Cartesian directions, giving a total of six vibrational degrees of freedom per unit cell. The lattice vectors are

$$\boldsymbol{a}_1 = a\left(\frac{3}{2}, \frac{\sqrt{3}}{2}\right), \qquad \boldsymbol{a}_2 = a\left(\frac{3}{2}, -\frac{\sqrt{3}}{2}\right), \tag{1}$$

where $a = 2.46, \text{Å}$ is the lattice constant corresponding to a nearest-neighbor bond length $a_{CC} = 1.42, \text{Å}$. Each atom has three first nearest neighbors and six second nearest neighbors.

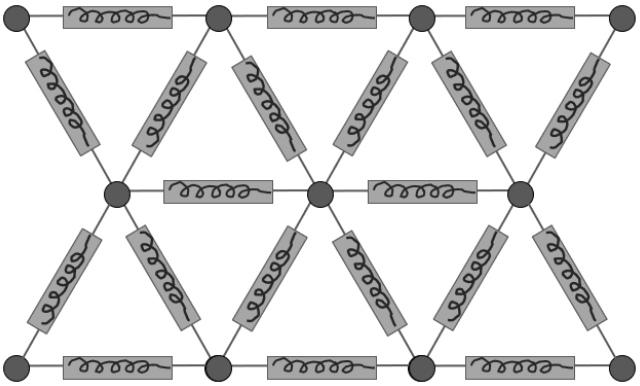

FIG. 1. Simple honeycomb model made of atoms and springs. Based on Simon's Oxford Solid State Basics **Problem 9.8 Phonons in 2D**.

B. Harmonic force-constant model

Atomic interactions are modeled using a physically motivated harmonic force-constant approach, following the framework of Yin, Liu, and Khvesyuk[1]. Nearest- and next-nearest-neighbor interactions are decomposed into radial and tangential components. The harmonic lattice

* efurman@haverford.edu

Hamiltonian is

$$H = \sum_{\ell,\alpha} \frac{\boldsymbol{p}_{\ell\alpha}^2}{2m_C} + \frac{1}{2} \sum_{\ell\alpha,\ell'\beta} \boldsymbol{u}_{\ell\alpha} \cdot \Phi_{\alpha\beta}(\ell - \ell') \cdot \boldsymbol{u}_{\ell'\beta}, \quad (2)$$

where $\boldsymbol{u}_{\ell\alpha}$ and $\boldsymbol{p}_{\ell\alpha}$ are the displacement and conjugate momentum of atom α in unit cell ℓ, m_C is the carbon atomic mass, and $\Phi_{\alpha\beta}$ is the force-constant tensor.

For a bond oriented along unit vector $\hat{\boldsymbol{e}} = (e_x, e_y)$, the in-plane force-constant matrix takes the form

$$K = \begin{pmatrix} \phi_r e_x^2 + \phi_t(1 - e_x^2) & (\phi_r - \phi_t) e_x e_y \\ (\phi_r - \phi_t) e_x e_y & \phi_r e_y^2 + \phi_t(1 - e_y^2) \end{pmatrix}. \quad (3)$$

with separate parameters (ϕ_{r1}, ϕ_{t1}) and (ϕ_{r2}, ϕ_{t2}) for first and second neighbors. Out-of-plane (flexural) motion is described by a bending force constant ψ coupling the z displacements of neighboring atoms.

Out-of-plane (flexural) motion is modeled by a harmonic bending interaction between neighboring atoms. For a pair of atoms i and j, the bending energy is taken to be

$$U_{\text{bend}} = \frac{\psi}{2} \sum_{\langle i,j \rangle} (z_i - z_j)^2, \quad (4)$$

where z_i is the out-of-plane displacement of atom i and ψ is the flexural force constant. This interaction contributes only to the zz block of the dynamical matrix and leads to a quadratic ZA dispersion $\omega_{\text{ZA}}(\mathbf{k}) \propto k^2$ at long wavelengths, as required by rotational invariance in two dimensions.

For my models, the force constants were initially based on Falkovsky[2], and were then tuned to reproduce the experimental LO/TO phonon frequency at the Γ point ($\sim 1580, \text{cm}^{-1}$), while maintaining physically reasonable ratios between parameters. For the full model:

- First in-plane: $\phi_r = 210.0$ N/m, $\phi_t = 125.0$ N/m
- Second in-plane: $\phi_r = 55.0$ N/m, $\phi_t = 15.0$ N/m
- Out-of-plane bending: $\psi = 40.0$ N/m

No artificial scaling factors are applied to the heat capacity; all temperature dependence arises from quantum statistics.

C. Dynamical matrix

Assuming plane-wave solutions

$$\boldsymbol{u}_{\ell\alpha}(t) = \boldsymbol{\epsilon}_\alpha(\boldsymbol{k}) e^{i(\boldsymbol{k} \cdot \boldsymbol{R}_\ell - \omega t)}, \quad (5)$$

the equations of motion reduce to the eigenvalue problem

$$\sum_\beta D_{\alpha\beta}(\boldsymbol{k}) \boldsymbol{\epsilon}_\beta = \omega^2(\boldsymbol{k}) \boldsymbol{\epsilon}_\alpha, \quad (6)$$

where the 6×6 dynamical matrix is

$$D_{\alpha\beta}(\boldsymbol{k}) = \frac{1}{m_C} \sum_{\boldsymbol{R}} \Phi_{\alpha\beta}(\boldsymbol{R}) e^{i\boldsymbol{k} \cdot \boldsymbol{R}}. \quad (7)$$

Diagonalization yields six phonon branches: LA, TA, LO, TO, ZA, and ZO.

D. Numerical methods and Brillouin-zone sampling

The dynamical matrix is implemented numerically in Python using NumPy. Phonon dispersions are computed along the high-symmetry path $\Gamma \to M \to K \to \Gamma$ using a linear interpolation of wavevectors.

For thermodynamic calculations, the two-dimensional Brillouin zone is sampled using a uniform mesh in reciprocal-lattice coordinates (k_1, k_2), mapped to Cartesian wavevectors via

$$\boldsymbol{k} = k_1 \boldsymbol{b}_1 + k_2 \boldsymbol{b}_2, \quad (8)$$

where $\boldsymbol{b}_1$ and $\boldsymbol{b}_2$ are the reciprocal lattice vectors. Points lying outside the first Brillouin zone are discarded. Typical calculations use $\mathcal{O}(10^3)$ $\boldsymbol{k}$-points, providing convergence of the heat capacity to within a few percent.

At each sampled $\boldsymbol{k}$, the dynamical matrix is diagonalized using a Hermitian eigensolver, yielding phonon frequencies $\omega_s(\boldsymbol{k})$. These frequencies are converted to energies $E_s(\boldsymbol{k}) = \hbar\omega_s(\boldsymbol{k})$ and used directly in the Bose–Einstein heat-capacity expression. The Brillouin-zone sum is evaluated numerically, and the temperature derivative is performed analytically, ensuring numerical stability.

This approach preserves the correct quantum suppression of high-frequency phonons at moderate temperatures ($T \ll T_{\text{Debye}}$) and recovers the classical Dulong–Petit limit at $T \gg T_{\text{Debye}}$ without any ad hoc corrections.

III. CALCULATIONS OF THE HEAT CAPACITY

A. Phonon internal energy

Phonons are bosonic excitations with occupation number given by the Bose–Einstein distribution

$$n_B(\omega) = \frac{1}{e^{\beta\hbar\omega} - 1}, \quad (9)$$

where $\beta = 1/(k_B T)$. The total internal energy of the lattice is

$$U(T) = \sum_{\boldsymbol{k},s} \hbar\omega_s(\boldsymbol{k}) \left[n_B(\omega_s(\boldsymbol{k})) + \frac{1}{2} \right]. \quad (10)$$

The zero-point energy term does not contribute to the heat capacity and is dropped in what follows.

B. Heat capacity

The heat capacity at constant volume is defined as

$$C_V = \left(\frac{\partial U}{\partial T}\right)_V . \tag{11}$$

Taking the derivative explicitly gives

$$C_V = k_B \sum \boldsymbol{k}, s \left(\frac{\hbar\omega_s(\boldsymbol{k})}{k_B T}\right)^2 \frac{e^{\hbar\omega_s(\boldsymbol{k})/k_B T}}{\left(e^{\hbar\omega_s(\boldsymbol{k})/k_B T} - 1\right)^2}. \tag{12}$$

In practice, the sum over $\boldsymbol{k}$ is replaced by a numerical integration over the first Brillouin zone.

C. Low-temperature behavior and ZA modes

For acoustic modes with linear dispersion $\omega \propto k$, the two-dimensional phonon density of states scales as $g(\omega) \propto \omega$, leading to $C_V \propto T^2$. However, the ZA mode has a quadratic dispersion $\omega \propto k^2$, implying a constant low-frequency density of states. As a result, the ZA contribution dominates the low-temperature heat capacity and produces characteristic T^2 scaling with a much larger prefactor.

IV. RESULTS

The phonon dispersions computed from the dynamical matrix reproduce the expected qualitative structure of graphene's spectrum.

A. Planar Model

For the planar model (atoms constrained to in-plane motion), there are four phonon branches. At the Γ point (zone center), two degenerate acoustic modes appear at 0 cm^{-1}, and two degenerate optical modes at 412.25 cm^{-1}. At the K point (Dirac point), one acoustic mode reaches zero while the other acoustic mode and an optical mode meet at 291.51 cm^{-1}, forming the characteristic Dirac cone where the acoustic and optical branches touch. At the M point, all four modes are non-degenerate, spanning 0–412 cm^{-1}.

Only three branches appear visually in the dispersion plot because the two acoustic modes overlap at Γ, and one acoustic and one optical mode meet at K. The top optical branch remains nearly flat at ~ 412 cm^{-1} throughout, consistent with the simple nearest-neighbor planar model. However, the planar model fails to reproduce the correct low-temperature heat capacity scaling: without flexural modes, it does a poor job fitting the expected $C \propto T^2$ behavior.

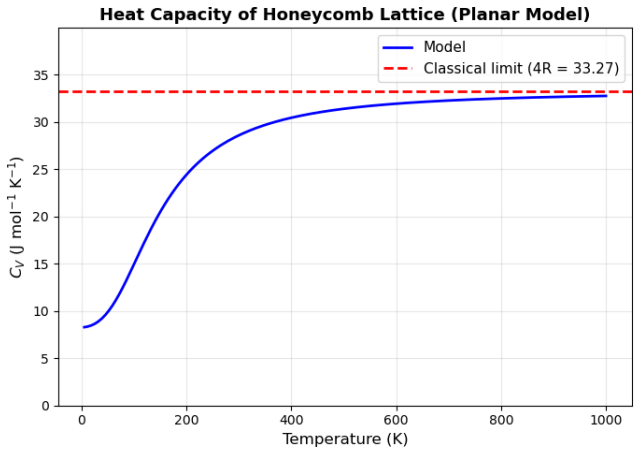

FIG. 2. Molar heat capacity for the planar graphene model. The heat capacity approaches the classical Dulong–Petit limit of $C = 4R$ at high temperatures.

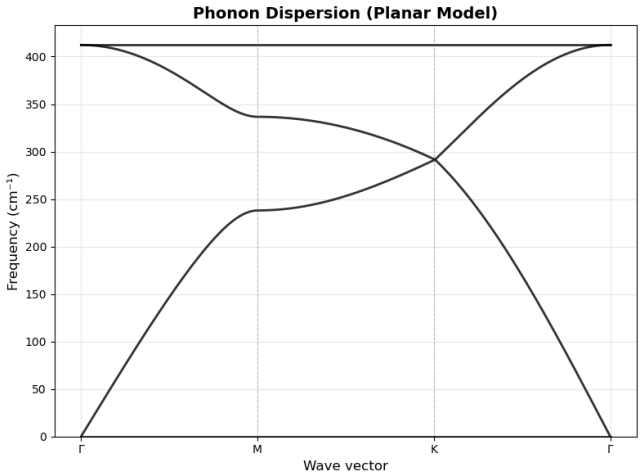

FIG. 3. Phonon dispersion for the planar graphene model. Four branches are present, with degenerate acoustic and optical modes at the Γ point. Only three branches are visually distinct due to overlapping modes at Γ and the Dirac point at K.

B. A More Physical Model

The full model includes out-of-plane motion and yields six branches, incorporating the flexural ZA and ZO modes. The ZA branch exhibits quadratic dispersion near the Γ point, leading to correct low-temperature behavior. The heat capacity calculated with the full model shows a much better agreement with the expected T^2 scaling at low temperatures and naturally rises toward the classical Dulong–Petit limit of $3R$ per mole of atoms at high temperatures (heat capacity approaches $6R$ here, because there are two atoms per unit cell). Quantitatively, the harmonic model overestimates the room-temperature heat capacity, yielding values around

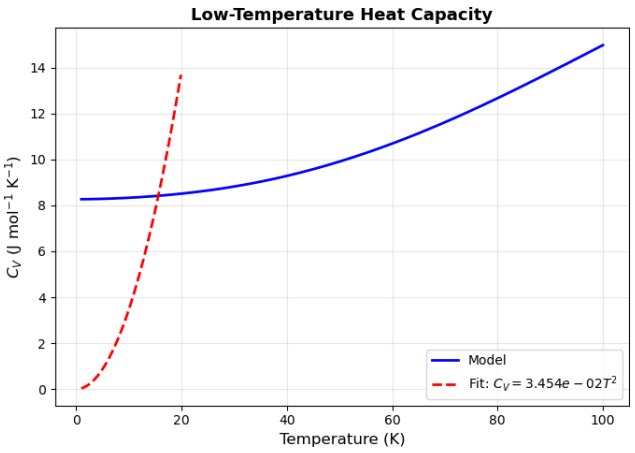

FIG. 4. Low-temperature behavior of the planar graphene model. The heat capacity does not follow the expected T^2 trend due to the absence of out-of-plane ZA modes.

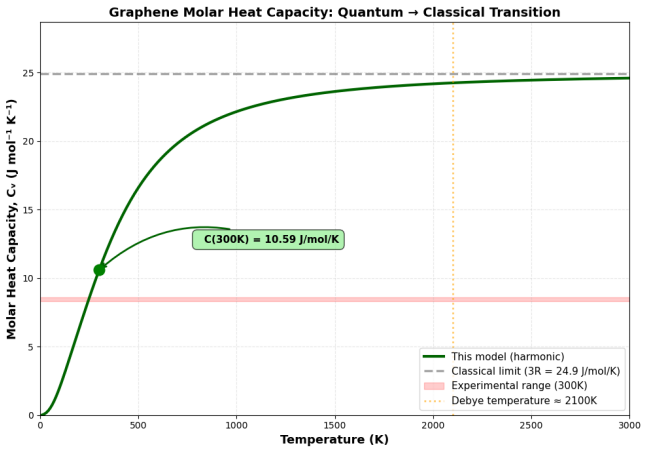

FIG. 5. Molar heat capacity for the full graphene model including flexural ZA and ZO modes. At low temperatures, the heat capacity exhibits the expected T^2 dependence, while at high temperatures it approaches the classical Dulong–Petit limit of $C = 6R$.

10.6 J mol^{-1} K^{-1}, compared with experimental values of 8.3–8.6 J mol^{-1} K^{-1}. This overestimate is expected from the harmonic approximation and arises primarily from neglecting anharmonicity and thermal expansion, not from an error in the model itself.

At 300 K (well below the Debye temperature of $\sim$ 2100 K), high-frequency phonons are only partially excited, yielding $C_v \sim 0.42 \times 3R$, which is physically expected. At 3000 K (classical regime), the model correctly recovers $C_v \sim 3R$.

Overall, the planar model correctly captures the in-plane phonon structure, including the Dirac point at K, but fails at low temperatures due to missing flexural modes. The full model, by including the ZA and ZO branches, reproduces both the correct low-T T^2 scaling and the qualitative features of the phonon dispersion and heat capacity across temperatures.

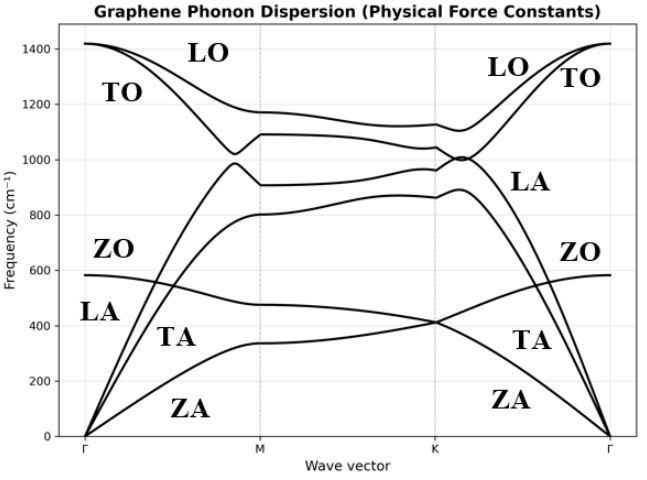

FIG. 6. Phonon dispersion for the full graphene model. Six branches are present, including the out-of-plane flexural ZA and ZO modes. The ZA branch exhibits quadratic dispersion near the Γ point.

C. K-point Convergence

A systematic k-point convergence study was performed to ensure that the computed phonon dispersions and heat capacities are independent of Brillouin zone sampling. Figure 9 shows the relative error of the heat capacity as a function of k-mesh density, demonstrating that a 50×50 mesh (2244 k-points) provides sufficient accuracy (<1% error) for production calculations. Figure 8 shows that increasing the mesh density has minimal effect on the computed C while significantly increasing computational cost. Meshes 60×60 and above provide reasonable results (<0.1% error).

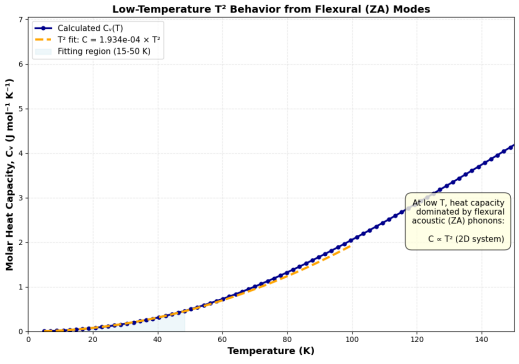

FIG. 7. Low-temperature behavior of the full graphene model. The heat capacity follows the expected T^2 trend due to the presence of low-frequency flexural ZA modes.

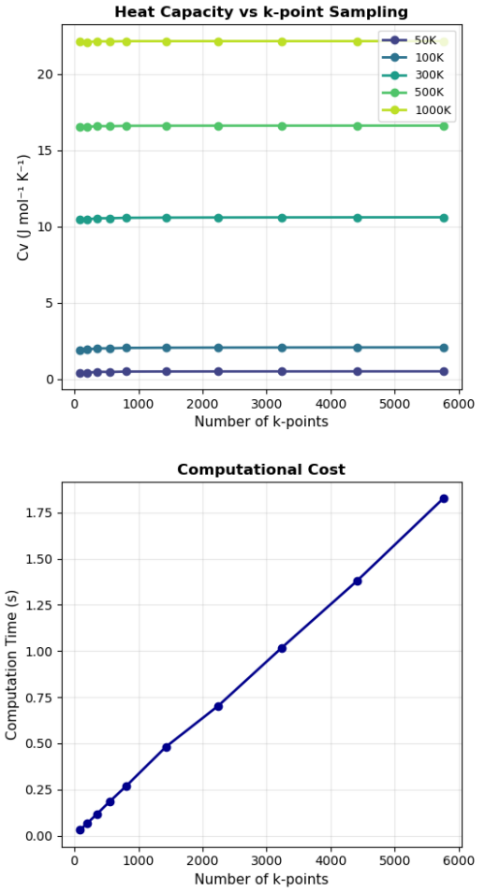

FIG. 8. Molar Heat Capacity and Computation Time(s) vs. k-point sampling. Larger grids slightly increase computational time with negligible effect on the calculated heat capacity.

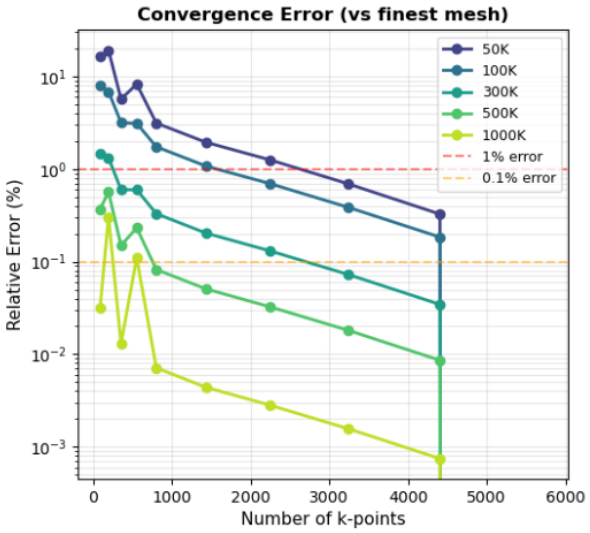

FIG. 9. Relative error in molar heat capacity vs. number of k-points. The error drops below 1% for $n_k \gtrsim 354$ (20×20 mesh) and below 0.1% for $n_k \gtrsim 5756$ (80×80 mesh).

V. CONCLUSIONS

We have shown that a simple harmonic lattice model is sufficient to capture the essential qualitative features of graphene's heat capacity. In particular, the inclusion of flexural ZA modes is crucial for reproducing the enhanced low-temperature behavior characteristic of two-dimensional membranes. At the same time, purely harmonic models systematically overestimate the heat capacity at higher temperatures, highlighting the importance of anharmonic effects such as phonon–phonon interactions and thermal expansion.

Future work could improve quantitative agreement by incorporating more realistic force constants, including anharmonic terms, and extending the calculation to thermal conductivity using Boltzmann transport theory.

VI. ACKNOWLEDGEMENTS

I would like to thank Prof. Xuemei Cheng for her teaching and advising on this project.

[1] F. Yin, S. Liu, and V. I. Khvesyuk, in *AIP Conference Proceedings, IV International Scientific and Practical Symposium "Materials Science and Technology": MST-IV-2024*, Vol. 3347 (2025) p. 020033.
[2] L. A. Falkovsky, Phys. Lett. A **372**, 5189 (2008).